www.czasopisma.pan.pl PAN POLSKA AKADEMIA NAUK www.journals.pan.pl

Arch. Metall. Mater. **65** (2020), 1, 337-341

DOI: 10.24425/amm.2020.131735

GA EON KIM[1], TAE KYU KIM[1], SANGHOON NOH[1*]

DIFFERENCE OF MICROSTRUCTURES AND MECHANICAL PROPERTIES BETWEEN 9Cr-1W FERRITIC/MARTENSITIC STEEL AND ODS STEEL

Ferrtic/martensitic and ODS steels were fabricated by the mechanical alloying process, and their microstructures and mechanical properties were investigated. The 9Cr-1W and 9Cr-1W-0.3Ti-0.35Y_2O_3 (in wt.%) steels were prepared by the same fabrication process such as mechanical alloying, hot isostatic pressing, and hot rolling processes. A microstructural observation of these steels indicated that the Ti and Y_2O_3 additions to 9Cr-1W steel were significantly effective to refine the grain size and form nano-sized Y-Ti-O oxide particles. As a result, the tensile strengths at room and elevated temperatures were considerably enhanced. Considerable improvement of the creep resistances at 700°C was also evaluated. It is thus concluded that 9Cr-1W ODS steel with Ti and Y_2O_3 additions would be very effective in improving the mechanical properties especially at elevated temperatures.

Keywords: 9Cr-1W steel, oxide dispersion strengthening (ODS), grain refinement, nano-oxide particle, creep resistance

1. Introduction

The sodium cooled fast reactor is considered to be one of the next-generation nuclear systems with enhanced economics, stability, and reliability. For realization of this system, it is inevitable to develop the advanced structural material having both high strength and irradiation resistance at high temperatures [1,2]. Ferritic/martensitic (F/M) steel such as HT9 with 12Cr-1Mo is one of the good solutions because of excellent thermal conductivity and good swelling resistance. However, the available temperature range of F/M steel is limited up to 650°C, because tensile and creep strengths are dramatically decreased over this high temperature [3,4]. The oxide dispersion strengthened (ODS) steel is the most promising structural material because of excellent creep and irradiation resistance by uniformly distributed nano-oxide particles with a high density, which is extremely stable at high temperature in an F/M steel matrix [1,2]. The yttrium oxide is commonly introduced as a strengthening dispersoid in various ODS steels because of its excellent stability at high temperatures. As minor alloying elements, it is well known that titanium is significantly effective at improving the high temperature strength forming extremely fine and stable Y-Ti-O complex oxides [5]. To fabricate these unique microstructures, ODS steels are manufactured by mechanical alloying (MA) and hot consolidation processes, which does not accompany the liquid phase and eventually create the homogenous distribution of nano-oxide particles in fine grain structures. Therefore, microstructures and mechanical properties of ODS steels were decided by not only alloying elements, but solid-state fabrication processes.

In this study, to improve the tensile and creep strengths of the F/M steel at elevated temperatures, two kinds of steels with 9Cr-1W ODS steel and 9Cr-1W F/M steel without dispersoids were fabricated by same manufacturing processes including mechanical alloying, hot isostatic pressing, and hot rolling processes. The grain morphology, precipitate distribution, tensile properties, and creep strength were characterized and compared between the two steels.

2. Experimental

The nominal composition of ODS steel used in this study was Fe(bal.)-0.07C-9Cr-1W-0.3Ti-0.35Y_2O_3 in weight ratio. The chemical compositions are summarized in Table 1. The ODS steel was fabricated by MA and hot isostactic pressing (HIP) and hot rolling processes. Metallic raw powders and Y_2O_3 powder were mechanically alloyed by a high energy horizontal ball-mill apparatus, Simoloyer CM-20. Mechanical alloying atmosphere is thoroughly controlled in ultra-high purity argon (99.9999%) gas.

[1] KOREA ATOMIC ENERGY RESEARCH INSTITUTE, NUCLEAR MATERIALS DIVISION, 111, DAEDEOK-DAERO 989BEON-GIL, YUSEONG-GU, DAEJEON, REPUBLIC OF KOREA

* Corresponding author: shnoh@kaeri.re.kr

The MA was performed at an impeller rotation speed of 240 rpm for 40 h with a ball-to-powder weight ratio of 10:1. MA powders were then sieved and charged in a stainless steel capsule. All powder handling processes for the weighing, collecting, sieving, and charging were conducted in a completely controlled high purity argon atmosphere to prevent the oxygen contamination during the process. Sealed capsules were then degassed at 400°C below 5×10^{-4} torr for 3h. The HIP was carried out at 1150°C for 3 h at a heating rate of 5°C/min and following furnace cooling. Hot rolling at 1150°C was done in a fixed rolling direction for a plate shape with a total reduction rate of 65%. After the hot rolling processes, heat treatments with normalizing at 980°C for 60 min and a tempering at 760°C for 70 min were subsequently carried out. To investigate the effect of dispersed Ti and Y_2O_3 on mechanical properties, an F/M steel without Ti and Y_2O_3 dispersions was also fabricated with the same manufacturing processes. Steel samples were mechanically wet ground and chemically etched in a 5% aqua regia solution for 10 min to observe the microstructures by an optical microscope. The grain morphology was observed by FE-SEM after electro-polishing in a 5% $HClO_4$ + 95% methanol solution in vol. % at 18 V with 0.5mA at -50°C to remove the work hardened surface induced by mechanical buff-polishing. Extraction carbon replica methods with a mixture solution of 5% HNO_3 + 2% HF + 93% H_2O were employed for the sample fabrication to observe the precipitates by an FE-TEM. To evaluate the mechanical properties, tensile and creep rupture tests were carried out. Specimens for mechanical property evaluations were taken out by an electro-discharge machining in the rolling direction. Sheet-type tensile specimens whose gauge length was 25.4 mm, width was 3.7 mm, and thickness was 1 mm were used. Tensile tests were carried out at room temperature, 500 and 700°C in air at a strain rate of 3.3×10^{-4} s^{-1}. Creep rupture tests were carried out under a stress range of 120-250 MPa at 700°C in the air.

TABLE 1

Chemical composition of ODS and F/M steels (in wt.%)

Materials	Fe	C	Cr	W	Ti	V	Zr	Y	O
F/M steel	bal.	0.08	8.89	1.1	0.01	0.19	0.05	—	—
ODS steel	bal.	0.07	8.85	1.2	0.27	0.19	0.05	0.28	0.22

3. Results and discussion

3.1. Microstructural differences between 9Cr-1W ODS and F/M steels

The optical microscopic image of the ODS steels and F/M steel without Ti and Y_2O_3 additions are shown in Fig. 1, where the horizontal direction corresponds to the hot rolling direction. The microstructure of the F/M steel showed a typical tempered martensite with prior austenite grains (PAG) in 43 μm and fine lath grain structures. This is a representative in 9Cr-1Mo and 9Cr-2W heat resistant F/M steels [6,7]. The effect of Ti and Y_2O_3 additions in the 9Cr-1W steel gave a dramatic evolution in the microstructures. Homogeneous grain distributions were observed; however, its grain size and shape were too fine to be determined by the optical microscopy, as shown in Fig. 1(b). SEM micrographs of the grain morphology on F/M and ODS steels are presented in Fig. 2, where the horizontal direction corresponds to a hot rolling direction. The F/M steel has martensite lath grains with finely dispersed carbides along the grain boundaries, which are Fe, Cr, and W-rich carbides induced by tempering heat treatment at 760°C for 70 min [8]. In contrast to this, fine equiaxed and coarse elongated grains parallel to a hot rolling direction were co-existed in the 9Cr-1W ODS steel, as shown in Fig. 2(b). Ohtsuka and Kim defined that fine equiaxed grains are martensite and the elongated grains are ferrite which

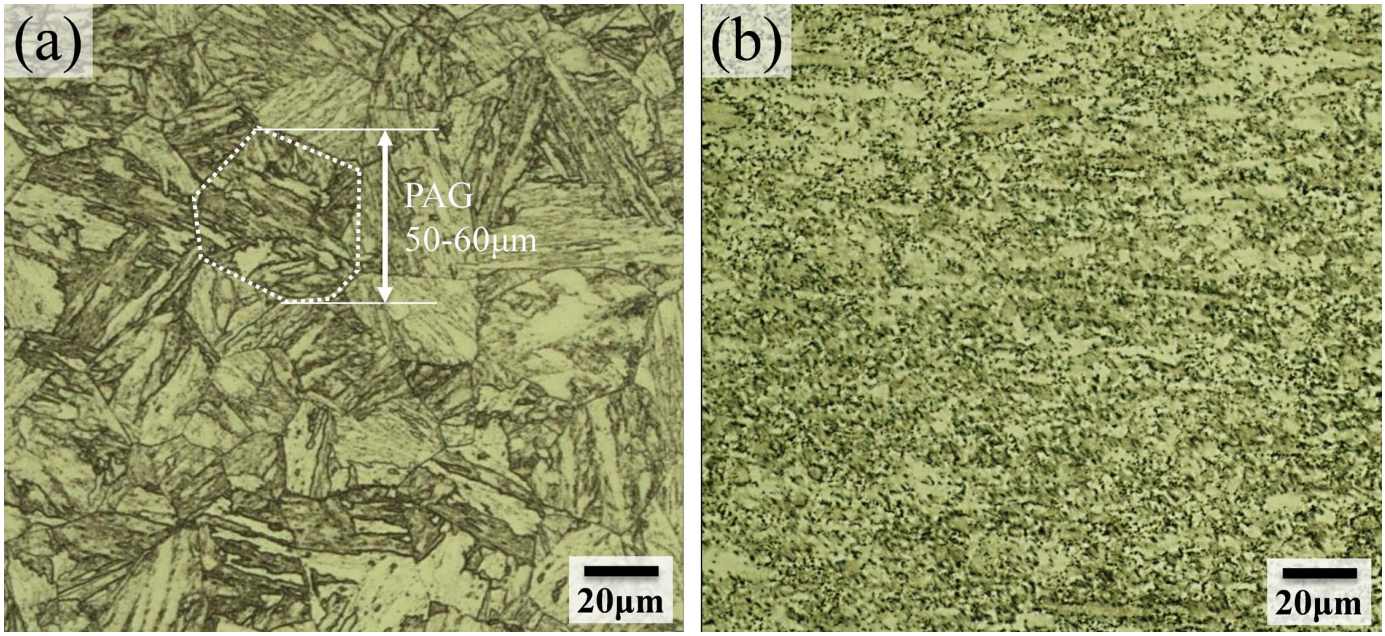

Fig. 1. Optical microscopic images on the (a) F/M steel and (b) ODS steel

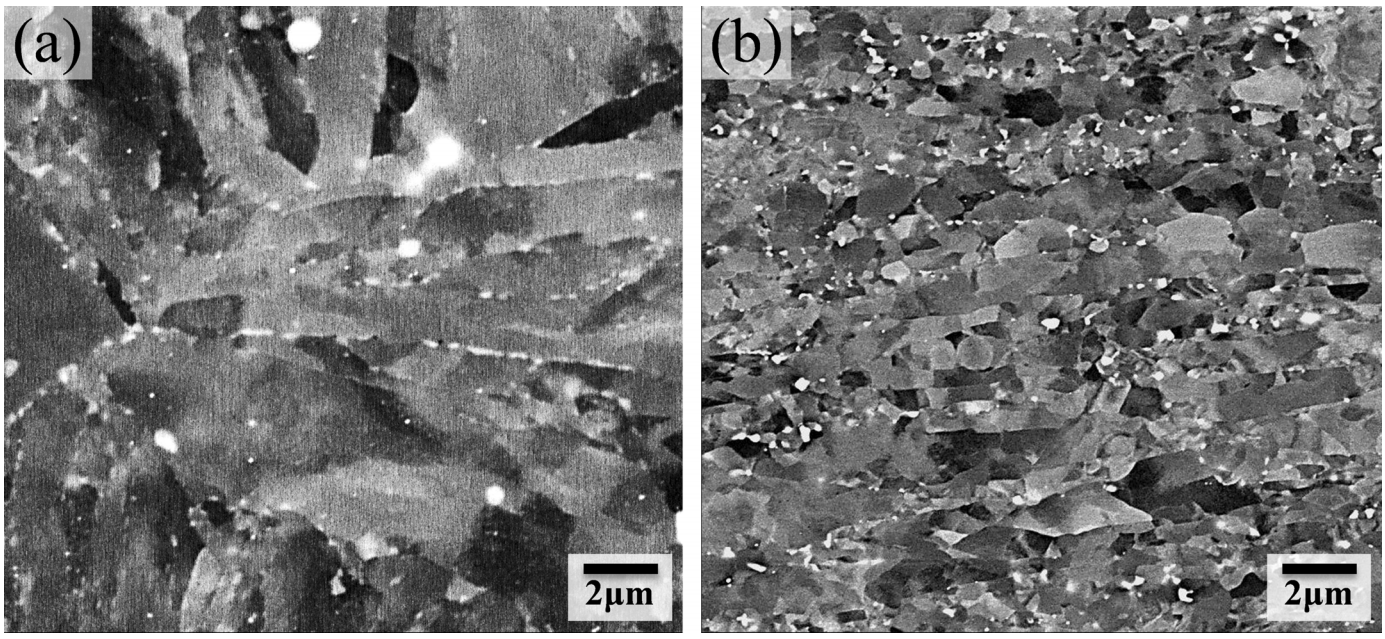

Fig. 2. SEM images on the (a) F/M steel and (b) ODS steel

untransformed into the gamma phase when the temperature is increased to 1150°C during the HIP process. This residual ferrite grains are due to a regionally high concentration of ferrite former elements such as Cr and W [9,10].

The precipitate morphology and distribution were also significantly different between F/M and ODS steels. Bright field TEM micrographs showing precipitates of F/M and ODS steels prepared by a carbon replica method are shown in Fig. 3. Precipitates in the F/M steel had various shapes of over 100 nm diameters, which were analyzed as coarse carbides, $M_{23}C_6$ (M = Cr, Fe, W, Mo). These carbides are usually precipitated in lath and lath grain boundaries in F/M steels, which were mainly induced by a tempering heat treatment at 760°C for 70 min after the HIP process [8]. In this case of ODS steel, extremely fine oxide particles of Y, Ti and O were homogeneously distributed on the matrix and grain boundaries, although coarse carbides were partially observed, as shown in Fig. 3(b). Chemical analysis by the TEM-EDS revealed that fine oxide particles were mainly consisted of Y, Ti, O and these should be $Y_2Ti_2O_7$ and Y_2TiO_5 complex oxides as previous report [11]. It is well known that the Y-Ti-O complex oxides are formed by a combination of Y_2O_3 and TiO_2 in Ti added ODS steels [5]. Kim et al. assumed that Y-Ti-O complex oxides are formed in the beginning stage of the hot consolidation process at above 900°C [10]. The grain growth and grain boundary migration suppression by uniformly distributed nano-oxide particles, which is called 'pinning ef-

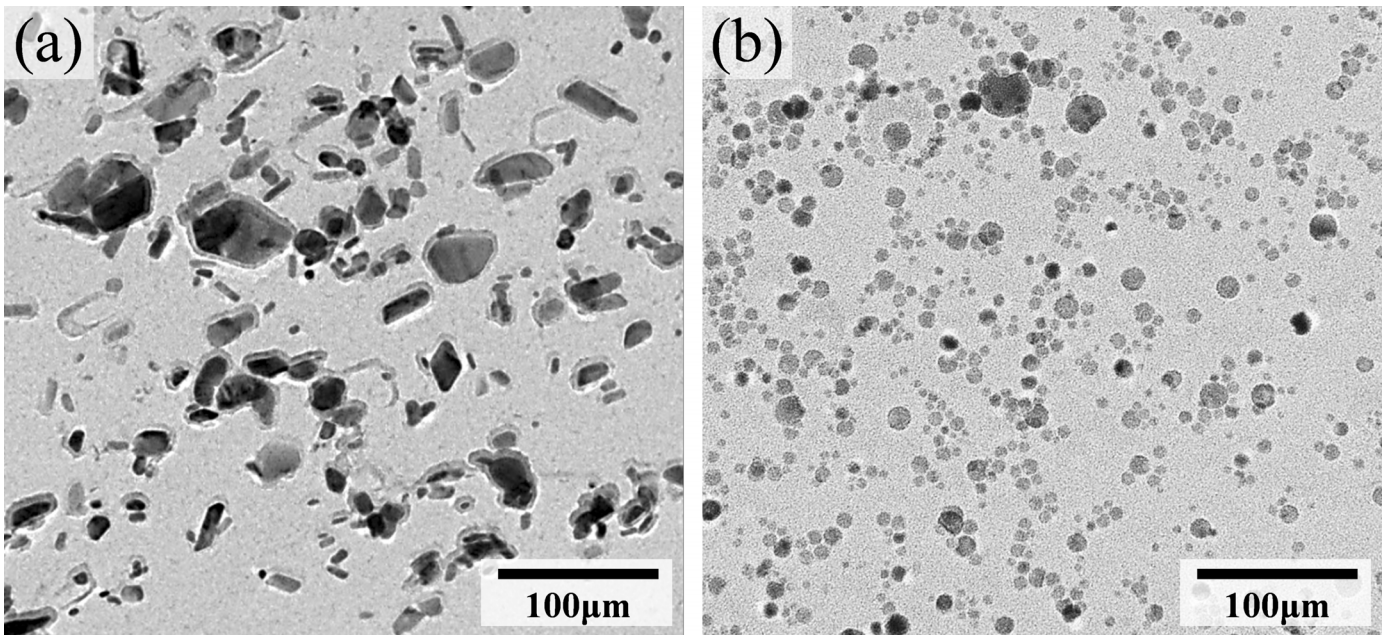

Fig. 3. Bright field TEM micrographs of (a) carbides in the F/M steel and (b) Y-Ti-O complex oxides in ODS steel

fect' during the hot consolidation process [12]. Thus, it was concluded that oxide particles play an important role for suppressions the grain growth during hot consolidation process. The microstructural differences of the F/M and ODS steels are summarized in Table 2.

TABLE 2

Microstructural differences between F/M and ODS steel

Microstructural features		F/M steel	ODS steel
Grains	Diameter	52.5 μm	1.8 μm
	Aspect ratio	1.0	1.22
Precipitates	Mean particle diameter	125 nm	8.4 nm
	Number density	—	$10.6\times10^{21}m^{-3}$
	Typical compositions	$M_{23}C_6$ Fe_2W	$M_{23}C_6$ Fe_2W $Y_2Ti_2O_7$, Y_2TiO_5

3.2. Mechanical property differences between 9Cr-1W ODS and F/M steels

Typical stress-strain curves by tensile tests for F/M steel and ODS steels at room and elevated temperatures are shown in Fig. 4. The tensile strengths of ODS steel were exceptionally higher than F/M steel in all tested temperatures. Ultimate tensile strengths (UTS) of ODS steel exhibited 1115, 710, and 335 MPa with a sufficient total elongation (TE) of 12.4, 18.4, and 13.5% at RT, 500, and 700°C, respectively. However, UTSs of the F/M steel was relatively poor, which corresponded to less than 60% of the ODS steel. Interestingly, the F/M steel showed a post yield softening with significantly lowered tensile strength at 700°C, whereas the ODS steel had a favorable tensile strength and elongation. This is due to the effects of dispersion hardening by nano-oxide particles in the grain and on the grain boundaries at high temperatures. Extremely fine grains of the ODS steel, as shown in Fig. 1(b) contributed to an improvement in the tensile strength by the grain boundary strengthening. Additionally, the nano-oxide particles were very stable even at a high temperature of up to 1300°C, and usually acts as an obstacle for the dislocation gliding when the material deforms, which is called 'Orowan strengthening' [13].

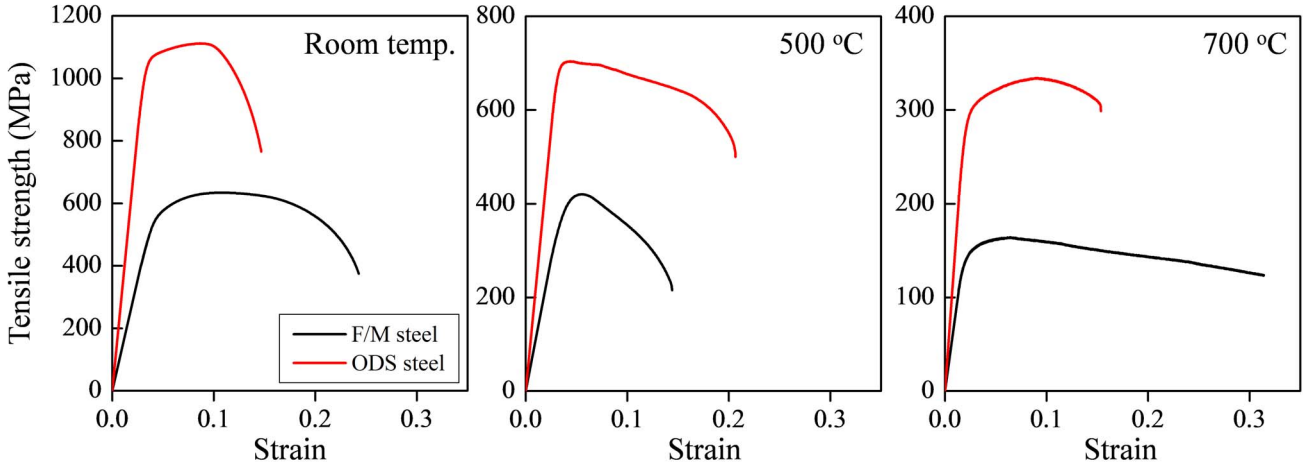

Fig. 4. Results on tensile tests of F/M and ODS steels at room and elevated temperatures

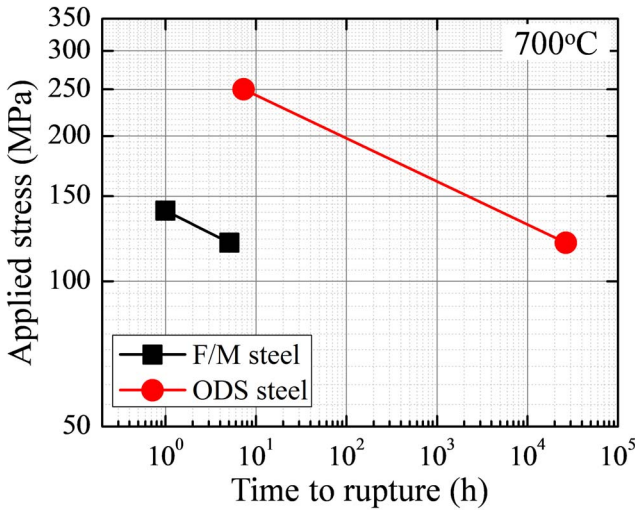

Fig. 5. Results on creep rupture tests of F/M and ODS steels at 700°C

Results of the creep rupture tests were plotted on the log-log scale, as shown in Fig. 5. The creep strength of ODS steels was more superior than that of F/M steel. While the creep rupture time of F/M steel reached 5.1 h, ODS steel had a longer rupture time for 26,585 h. The creep resistance of ODS steel overwhelmed that of F/M steel. As shown in the microstructures, Ti and Y_2O_3 additions in the ODS steel generated a homogenous distribution as well as fine diameters of nano-oxide particles. These microstructural features lead to an excellent creep rupture strength at 700°C.

4. Conclusions

The 9Cr-1W F/M and ODS steels were identically fabricated by the MA and HIP processes to evaluate the differences on the microstructures and mechanical properties. The

microstructure of 9Cr-1W F/M steel showed a typical tempered martensite with coarse carbides, mainly $M_{23}C_6$ in several tens of nm on the grain boundaries. In case of 9Cr-1W ODS steel, grain refinement occurred in the ODS steel owing to a uniform distribution of nano-sized complex oxide particles. This led to more superior tensile strength and creep resistance of the ODS steel than those of the F/M steel at room and elevated temperatures. Nano-oxide particles in ODS steel may play an important role for the suppression the grain growth during the hot consolidation process.

Acknowledgments

This work was supported by the National Research Foundation of Korea(NRF) grant funded by the Korea government(MSIT) (NRF-2017M2A8A4017639).

REFERENCES

[1] T.K. Kim, S. Noh, S.H. Kang, J.J. Park, H.J. Jin, M.K. Lee, J. Jang, C.K. Rhee, Nucl. Eng. Technol. **48**, 572 (2016).

[2] S. Ukai, T. Okuda, M. Fujiwara, T. Kobayashi, S. Mizuta, H. Nakashima, J. Nucl. Sci. Technol. **39**, 872 (2002).

[3] L. Thomas, J. Nucl. Mater. **133-134**, 149 (1985).

[4] F.A. Garner, M.B. Toloczko, B.H. Sencer, J. Nucl. Mater. **276**, 123 (2000).

[5] S. Ukai, T. Nishida, H. Okada, T. Okuda, M. Fujiwara, K. Asabe, J. Nucl. Sci. Technol. **34**, 256 (1997).

[6] T.K. Kim, J.H. Baek, C.H. Han, S.H. Kim, C.B. Lee, J. Nucl. Mater. **389**, 359 (2009).

[7] S. Triratna, F.A. Sultan, C. Indrajit, P.P. Gabriel, V.G. Michael, Metals **5**, 131 (2015).

[8] Y.B. Chun, D.W. Lee, S. Cho, C.K. Rhee, Mater. Sci. Eng. A, **645**, 286 (2015).

[9] S. Ohtsuka, S. Ukai, M. Fujiwara, T. Kaito, T. Narita, Mater. Trans. **46**, 487 (2005).

[10] S. Kim, S. Ohtsuka, T. Kaito, S. Yamashita, M. Inoue, T. Asayama, T. Shobu, J. Nucl. Mater. **417**, 209 (2011).

[11] M.J. Alinger, G.R. Odette, D.T. Hoelzer, J. Nucl. Mater. **329-333**, 382 (2004).

[12] R. Gao, T. Zhang, X.P. Wang, Q.F. Fang, C.S. Liu, J. Nucl. Mater. **444**, 462 (2014).

[13] A.J. Foreman, M.J. Markin, Philosophical Magazine **14**, 911 (1966).